# REDUNDANT-WAVELET WATERMARKING WITH PIXEL-WISE MASKING

Kristen M. Parker and James E. Fowler
*Department of Electrical and Computer Engineering*
*GeoResources Institute, Mississippi State ERC*
*Mississippi State University, Mississippi State, MS*

## ABSTRACT

*An algorithm is presented which implements image watermarking in the domain of an overcomplete, or redundant, wavelet transform. This algorithm expands on a previous method which employs a traditional, critically sampled wavelet transform coupled with perceptually-based watermark casting and optimal Neyman-Pearson detection. Specifically, in the proposed method, the redundancy inherent in the transform facilitates detection of perceptually salient texture local to a given spatial location and guides the placement of watermarking energy so as to minimize the impact on perceptual image quality. Additionally, the optimal detection strategy is adjusted to account for the overcompleteness of the transform. The performance of the proposed technique is compared to that of its critically sampled counterpart and greater robustness under attack by compression is observed.*

## 1. INTRODUCTION

Watermarking of images is becoming increasingly of interest in tasks such as copyright control, image identification, verification, and data hiding. Spread-spectrum watermarking [1], one of the most popular methods for image watermarking, embeds a white-noise watermark into transform coefficients of an image and verifies the presence of the watermark by measuring the correlation between the watermarked coefficients and the watermark sequence. It has been shown that the discrete wavelet transform (DWT) is an effective venue for the spread-spectrum method due to natural similarities between the space-frequency tiling of the DWT and the operating characteristics of the human visual system (HVS) [2].

As an alternative to the DWT, the redundant discrete wavelet transform (RDWT) [3–5] has also been considered for watermarking [6, 7]. In essence, the RDWT—often implemented as the *algorithme à trous* [3, 4]—removes the downsampling operation from the DWT to produce an overcomplete and shift-invariant transform. From a mathematical perspective, the RDWT is a frame expansion, and frame expansions have long been known to be robust to added noise. Specifically, white noise added in the transform domain results in significantly reduced noise power in the original signal domain due to the fact that the inverse frame operator is a pseudo-inverse that involves a projection onto the range space of the forward transform [8].

Intuitively, one would expect that the robustness to noise provided by frame expansions such as the RDWT would be ideally suited to the spread-spectrum watermarking procedure. Indeed, more watermarking energy can be accommodated in the RDWT domain for the same distortion incurred in the original signal domain as compared to traditional DWT-based watermarking. However, it has been shown that the same pseudo-inverse projection that decreases the noise power also results in a corresponding decrease in correlation-detector performance, such that overcomplete and complete transforms offer the same watermarking performance from a theoretical perspective [7].

Still, the redundancy provided by the RDWT can be exploited in ways other than for noise robustness. Since the redundancy in the transform facilitates the location of edges and other salient features in an image [9], it has been argued that the RDWT domain is well-suited for perceptually guiding the casting of watermarks [6]. In this paper, we demonstrate this advantage by adapting a well-known, perceptually-based watermarking method, originally formulated with the critically sampled DWT, to the overcomplete RDWT.

Specifically, in this paper, we modify the pixel-wise masking (PWM) technique pioneered by Barni *et al*. [2] for DWT-domain watermarking and deploy it in the RDWT domain. In doing so, we make modifications to both the PWM-DWT watermark-casting and watermark-detection procedures. For watermark casting, we develop a measure of local texture in the RDWT domain and use that measure to guide the casting of the watermark, increasing watermark strength in areas of high texture where the HVS is less sensitive to the added watermark. As in [2], we employ a cross-scale texture measure to gauge texture local to a given spatial position. However, our proposed RDWT-domain texture measure more accurately captures local texture since the equivalent DWT-based technique must consider increasingly larger spatial regions as resolution decreases due to the changing temporal sampling of the DWT. For watermark detection, we modify the blind correlation-detection process of PWM-DWT, adjusting the Neyman-Pearson detection formulation of [2] to account for the fact that detection takes place in the setting of an overcomplete transform. Experimental results show that our proposed PWM-RDWT technique is more robust to attack by compression than the original DWT-based technique of [2].

## 2. PWM-RDWT WATERMARKING

### 2.1. Watermark Casting

In spread-spectrum watermarking, the goal is to embed as much watermark information into an image as possible so as to maximize the correlation-detector performance while leaving the perceptual quality of the image unchanged. As a consequence, the guiding principle of perceptually-based spread-spectrum watermarking is that the watermark information should be placed in locations that are the least perceptible to the HVS. Locating those least-perceptible areas accurately is key to placing large amounts of watermark information into the image. We note that, as in [2], we watermark only the transform subbands with the highest resolution as a compromise between robustness and perceptual invisibility.

In the PWM-DWT method of Barni *et al*. [2], the perceptibility

This work was funded in part by the National Science Foundation under Grant No. CCR-0310864.

In *Proceedings of the International Conference on Image Processing*, vol. 1, Genoa, Italy, September 2005, pp. 685–688.

of each DWT coefficient is determined from the model of the HVS originating in [10]. This model consists of three components—orientation and level of detail, local brightness, and local texture—which are combined in a product expression which is then used as a weighting factor for the watermark information during watermark casting. The third factor in the product estimates image texture for a coefficient at scale $l$ located spatially at $(i, j)$ by examining the variance in co-located $2 \times 2$ blocks in each subband in the DWT,

$$\Xi(l,i,j) = \left[\sum_{k=0}^{3-l} \frac{1}{16^k} \sum_{\theta=0}^{2} \sum_{x=0}^{1} \sum_{y=0}^{1} \left[ I_{k+l}^{\theta}\left(y + \frac{i}{2^k}, x + \frac{j}{2^k}\right)\right]^2\right] \cdot \mathrm{Var}\left\{ I_3^3\left(y + \frac{i}{2^{3-l}}, x + \frac{j}{2^{3-l}}\right)\right\}_{x,y=0,1}, \quad (1)$$

where $I_l^{\theta}$ is the DWT subband at orientation $\theta$ and scale $l$.

As used in (1), fixed-size blocks in a DWT subband correspond to increasingly larger spatial areas in the original image as the resolution of the subband decreases ($l$ increases), resulting in the texture measure being less local for the lower-resolution subbands. Fig. 1(a) illustrates this effect in a two-scale DWT, wherein it can be seen that the fixed-sized blocks cover an increasingly larger spatial area as $l$ increases. Additionally, the size of the blocks that can be used in the texture estimation of (1) is limited in practice since the blocks should not become larger than the size of the lowest-resolution subbands when the number of scales of decomposition is large.

However, because the RDWT is not downsampled, the subbands have the same size as the original image for each level of decomposition; therefore, decreasing subband resolution does not increase the spatial area associated with a fixed-size block. Additionally, we can employ a larger block size with the current coefficient itself as the center (the $2 \times 2$ blocks of PWM-DWT are offset relative to the current coefficient). Consequently, more accurate estimation of local texture activity surrounding the current coefficient can be achieved in the RDWT domain. In our proposed PWM-RDWT method, we replace (1) with

$$\Xi(l,i,j) = \left[\sum_{k=0}^{3-l} \frac{1}{16^k} \sum_{\theta=0}^{2} \sum_{x=-n}^{n} \sum_{y=-n}^{n} \left[ I_{k+l}^{\theta}\left(y + i, x + j\right)\right]^2\right] \cdot \mathrm{Var}\left\{ I_3^3\left(y + i, x + j\right)\right\}_{x,y=-n,\ldots,n}, \quad (2)$$

wherein we have assumed $n \times n$ blocks centered about the current coefficient. Fig. 1(b) illustrates that fixed-sized blocks in an RDWT correspond to the same spatial area in each subband, in contrast to the varying spatial area of the fixed-sized blocks in the DWT of Fig. 1(a).

### 2.2. Watermark Detection

In the blind watermark-detection technique of PWM-DWT [2], a Neyman-Pearson approach is adopted to minimize the probability of missed detection of the watermark given a fixed false-detection probability. In [2], the Neyman-Pearson detection threshold was determined to be

$$T_\rho = 3.97\sqrt{2\sigma_\rho^2} \quad (3)$$

for a false-detection probability of $10^{-8}$ under the assumption that the correlation-detector output, $\rho$, is normally distributed, with $\sigma_\rho^2$ being the variance of $\rho$ when the image is watermarked with some watermark other than the target watermark. In [7], the case of watermarking with a tight-frame expansion was considered, and it was determined that the Neyman-Pearson threshold for the tight-frame case, $T'_\rho$, is related to the Neyman-Pearson threshold for the critically-sampled case, $T_\rho$, as

$$T'_\rho = \sqrt{A}\, T_\rho, \quad (4)$$

where $A$ is the frame bound for the tight-frame expansion, and it is assumed that the false-detection probability is the same in both cases.

For our PWM-RDWT technique, we observe that the RDWT is a tight frame only when one level of decomposition is used [11, 12]. However, if the watermark is cast into only the highest-resolution subbands of the transform (as was done in the PWM-DWT approach of [2] and in our implementation of PWM-RDWT), then the Neyman-Pearson threshold for PWM-RDWT will be given approximately by (4) with $A = 4$ for a 2D transform and $T_\rho$ being the threshold used for PWM-DWT as given by (3). Below, we verify experimentally the validity of this approximation to the optimal threshold.

## 3. RESULTS

We compare our proposed PWM-RDWT to the PWM-DWT technique of [2]. For both techniques, we adjust the watermark strength to the level of just-noticeable distortion (JND), and evaluate watermark detection using correlation-based detection with a Neyman-Pearson threshold as described above. All transforms are implemented using the popular biorthogonal 9/7 wavelet [13] with symmetric extension. We initially fix the block size for PWM-RDWT to $n = 3$.

For PWM-RDWT, the detector response, correlation $\rho$, is calculated for 1000 different watermarks—only one being the correct embedded watermark—and the resulting detector responses shown in Fig. 2. The magnitude of the correct watermark is comparatively much larger than any of the "incorrect" watermarks.

Fig. 3 compares the detector response to the correct watermark for PWM-RDWT and PWM-DWT under attack with SPIHT [14] compression. Also shown are the Neyman-Pearson thresholds given by (4) and (3), respectively. As is evident in Fig. 3, the PWM-DWT detector response falls below its optimal threshold at a compression ratio of 61, while PWM-RDWT does not cross its threshold until a compression ratio of 130. The amount of watermark information embedded using the PWM-RDWT method was considerably larger due to the more accurate locating of pixels masked by the HVS.

Fig. 4 demonstrates the validity of (4) as an approximation to the ideal threshold. We see that the second-highest detector response is consistently below the approximate threshold (4) as the compression ratio varies.

Finally, we consider a block size of $n = 5$ in Fig. 5. As can be seen, increasing the block size results in slightly greater robustness (a compression ratio of roughly 140 can be withstood using a block size of $n = 5$). We have also tested larger block sizes, but did not observe further improvement beyond $n = 5$.

## 4. CONCLUSIONS

In this paper, we have adapted the well-known PWM approach of [2] to the context of a redundant transform by modifying the approach to texture estimation which guides watermark casting and

In *Proceedings of the International Conference on Image Processing*, vol. 1, Genoa, Italy, September 2005, pp. 685–688.

by accommodating the overcomplete nature of the transform in the Neyman-Pearson detection threshold. The proposed RDWT-domain texture measure more accurately estimates local texture activity since the equivalent DWT-based technique must consider increasingly larger spatial regions as resolution decreases due to the changing temporal sampling of the DWT. The resulting PWM-RDWT technique is shown to produce increased watermark robustness as compared to the original PWM-DWT approach in the face of a compression attack.

## 5. REFERENCES


[1] I. J. Cox, J. Killian, F. T. Leighton, and T. Sharmoon, "Secure spread spectrum watermarking for multimedia," *IEEE Transactions on Image Processing*, vol. 6, no. 12, pp. 1673–1687, December 1997.

[2] M. Barni, F. Bartolini, and A. Piva, "Improved wavelet-based watermarking through pixel-wise masking," *IEEE Transactions on Image Processing*, vol. 10, no. 5, pp. 783–791, May 2001.

[3] M. Holschneider, R. Kronland-Martinet, J. Morlet, and P. Tchamitchian, "A real-time algorithm for signal analysis with the help of the wavelet transform," in *Wavelets: Time-Frequency Methods and Phase Space*, J.-M. Combes, A. Grossman, and P. Tchamitchian, Eds. Berlin, Germany: Springer-Verlag, 1989, pp. 286–297, proceedings of the International Conference, Marseille, France, December 14–18, 1987.

[4] P. Dutilleux, "An implementation of the "algorithme à trous" to compute the wavelet transform," in *Wavelets: Time-Frequency Methods and Phase Space*, J.-M. Combes, A. Grossman, and P. Tchamitchian, Eds. Berlin, Germany: Springer-Verlag, 1989, pp. 298–304, proceedings of the International Conference, Marseille, France, December 14–18, 1987.

[5] M. J. Shensa, "The discrete wavelet transform: Wedding the à trous and Mallat algorithms," *IEEE Transactions on Signal Processing*, vol. 40, no. 10, pp. 2464–2482, October 1992.

[6] J.-G. Cao, J. E. Fowler, and N. H. Younan, "An image-adaptive watermark based on a redundant wavelet transform," in *Proceedings of the International Conference on Image Processing*, vol. 2, Thessaloniki, Greece, October 2001, pp. 277–280.

[7] L. Hua and J. E. Fowler, "A performance analysis of spread-spectrum watermarking based on redundant transforms," in *Proceedings of the IEEE International Conference on Multimedia and Expo*, vol. 2, Lausanne, Switzerland, August 2002, pp. 553–556.

[8] I. Daubechies, *Ten Lectures on Wavelets*. Philadelphia, PA: Society for Industrial and Applied Mathematics, 1992.

[9] S. Mallat and S. Zhong, "Characterization of signals from multiscale edges," *IEEE Transactions on Pattern Analysis and Machine Intelligence*, vol. 14, no. 7, pp. 710–732, July 1992.

[10] A. S. Lewis and G. Knowles, "Image compression using the 2-D wavelet transform," *IEEE Transactions on Image Processing*, vol. 1, no. 2, pp. 244–250, April 1992.


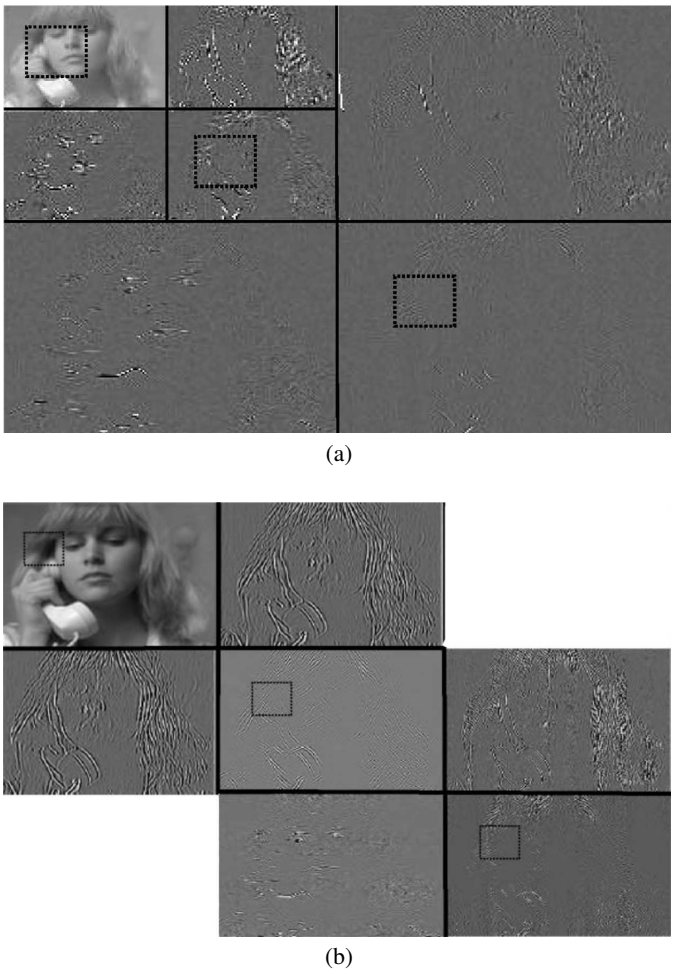

Figure 1: Spatial area of fixed-size blocks, (a) two-scale DWT, (b) two-scale RDWT.


[11] J. E. Fowler, "The redundant discrete wavelet transform and additive noise," *IEEE Signal Processing Letters*, vol. 12, no. 9, pp. 629–632, September 2005.

[12] ——, "The redundant discrete wavelet transform and additive noise," Mississippi State ERC, Mississippi State University, Tech. Rep. MSSU-COE-ERC-04-04, March 2004.

[13] M. Antonini, M. Barlaud, P. Mathieu, and I. Daubechies, "Image coding using wavelet transform," *IEEE Transactions on Image Processing*, vol. 1, no. 2, pp. 205–220, April 1992.

[14] A. Said and W. A. Pearlman, "A new, fast, and efficient image codec based on set partitioning in hierarchical trees," *IEEE Transactions on Circuits and Systems for Video Technology*, vol. 6, no. 3, pp. 243–250, June 1996.

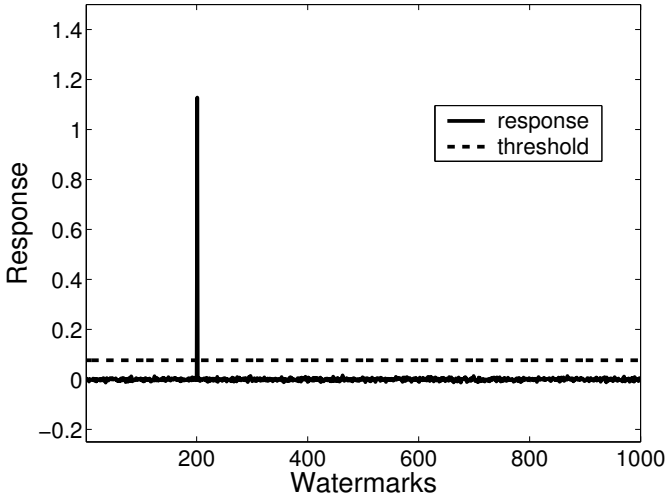


Figure 2: Detector response for 1000 different watermarks for the "Lenna" image with PWM-RDWT; $n = 3$.

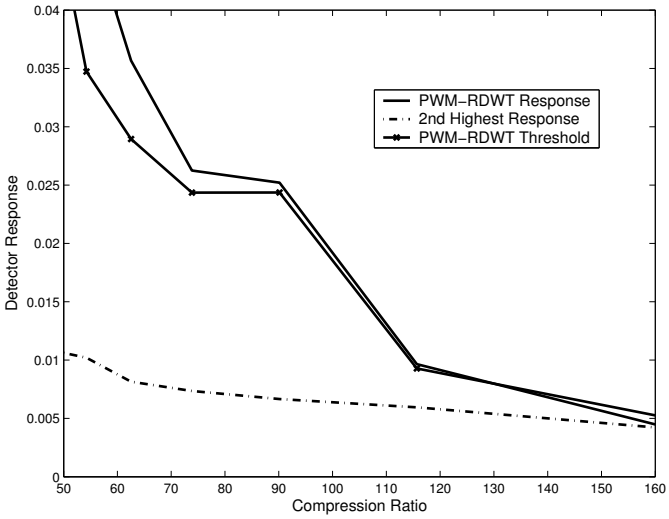


Figure 4: Detector response and second-highest response for the "Lenna" image under compression with SPIHT [14]; $n = 3$.

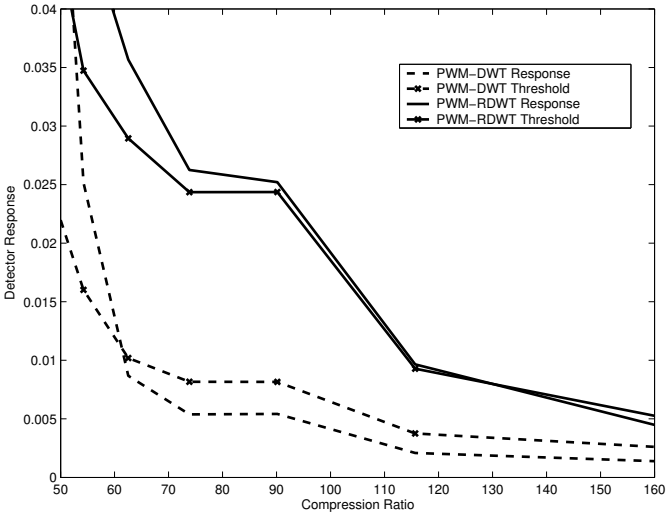


Figure 3: Detector performance for PWM-RDWT and PWM-DWT [2] for the "Lenna" image under compression with SPIHT [14]; $n = 3$.

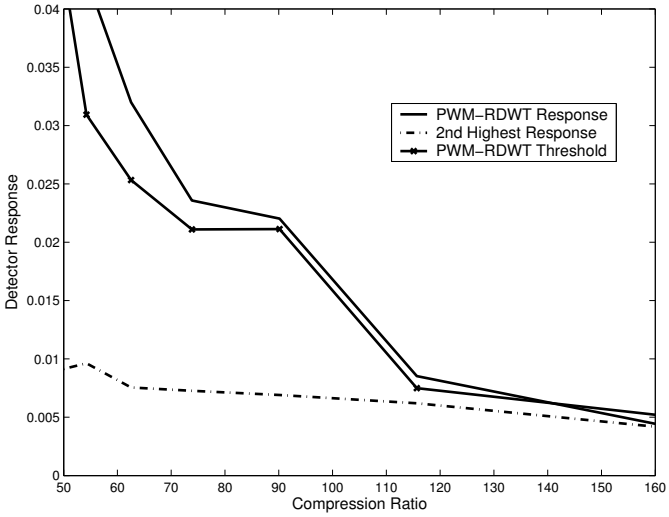


Figure 5: Detector response and second-highest response for the "Lenna" image under compression with SPIHT [14]; $n = 5$